Dark lump excitations in superfluid Fermi gases*

Xu Yan-Xia(徐艳霞) and Duan Wen-Shan(段文山)†

Key Laboratory of Atomic and Molecular Physics & Functional Materials of Gansu Province, College of Physics and Electronic Engineering, Northwest Normal University, Lanzhou 730070, China

(Received 19 March 2012; revised manuscript received 26 April 2012)

We study the linear and nonlinear properties of two-dimensional matter-wave pulses in disk-shaped superfluid Fermi gases. A Kadomtsev–Petviashvili I (KPI) solitary wave has been realized for superfluid Fermi gases in the limited cases of Bardeen–Cooper–Schrieffer (BCS) regime, Bose–Einstein condensate (BEC) regime, and unitarity regime. One-lump solution as well as one-line soliton solutions for the KPI equation are obtained, and two-line soliton solutions with the same amplitude are also studied in the limited cases. The dependence of the lump propagating velocity and the sound speed of two-dimensional superfluid Fermi gases on the interaction parameter are investigated for the limited cases of BEC and unitarity.

Keywords: superfluid Fermi gas, deep BEC regime, unitarity, dark lump excitation

PACS: 52.35.Sb, 52.25.Xz, 05.45.Yv **DOI:** 10.1088/1674-1056/21/11/115202

1. Introduction

Since the experimental realization of ultracold Fermi superfluid from the Bardeen–Cooper–Schrieffer (BCS) to Bose–Einstein condensate (BEC),[1,2] BCS–BEC crossover has become an active research area for both experimental[3,4] and theoretical work,[5−7] provided a new type of macroscopic quantum fluid, and led to an enormous progress on the study of trapped, strongly interacting fermions. On the basis of the excellent theoretical[8−15] and experimental[16,17] work done on the BEC, many significant investigations have been generalized to the superfluid Fermi gases, such as the propagation of sound and supersonic bright solitons,[18] bulk and collective properties,[19,20] macroscopic quantum tunneling,[21] the Josephson effect throughout the BCS–BEC crossover,[22] and vortex solitons and their propagation.[23−25] The research on BCS–BEC crossover is not only of basic interest in condensed matter physics, but also closely related to the understanding of the physical mechanism of high-$T_{\rm C}$ superconductivity.[26]

The experimental availability of BCS–BEC crossover in ultracold fermionic atomic gases allows one to change the system from a BCS regime to a BEC regime in a controllable way via tuning the s-wave scattering length $a_{\rm sc}$ using the Feshbach resonance technique:[27] when $a_{\rm sc} > 0$ ($a_{\rm sc} < 0$), the system is in the BEC (BCS) regime. By introducing a dimensionless interaction parameter $\eta = 1/k_{\rm F}a_{\rm sc}$, with $k_{\rm F} = (3\pi^2 n)^{1/3}$ being the Fermi wave number and n being the atomic density, several different Fermi superfluid regimes can be distinguished. For the BCS (BEC) regime, $\eta < -1$ ($\eta > 1$); for the BCS–BEC crossover, $-1 < \eta < 1$; for the BCS (BEC) limit, $\eta = -\infty$ ($\eta = +\infty$); for the unitarity limit, $\eta = 0$. Thus, the rich physical properties of superfluid Fermi gases in different regimes can be investigated with the use of an approximate description for the low-temperature behaviour of a condensate.[28−30] However, even if the dynamic properties of the ultracold Fermi superfluid have been widely studied[31,32] in both one- and two-dimensional (2D) superfluid Fermi gases, especially in spite of intensive research on dark solitons,[33−35] there are still many questions to be solved, including the dark lump excitation of the system.

In this paper, we study the linear and nonlinear properties of 2D superfluid Fermi gases. Kadomtsev–Petviashvili I (KPI) solitary wave is investigated for the BEC regime, BCS regime, and unitarity regime by following the procedure of Huang.[36−39] We also investigate how the interaction parameter η affects the dynamic properties of the superfluid Fermi gases. Some interesting conclusions are obtained.

*Project supported by the National Natural Science Foundation of China (Grant Nos. 91026005 and 11047010) and the Natural Science Foundation of Northwest Normal University of China (Grant No. NWNU-KJCXGC-03-48).

†Corresponding author. E-mail: Duanws@nwnu.edu.cn

© 2012 Chinese Physical Society and IOP Publishing Ltd

2. Quasi-2D approximation for order parameter equation and basic set of KPI equation

2.1. Quasi-2D approximation for order parameter equation

The dynamic behaviour of superfluid Fermi gas at low temperature can be approximately given by[40]

$$\mathrm{i}\hbar\frac{\partial\Psi}{\partial t}=\Big[-\frac{\hbar^2}{2m}\boldsymbol{\nabla}^2+V_{\rm ext}(r)+\mu\Big]\Psi, \tag{1}$$

where μ is the bulk chemical potential of the system. In limited regimes, it can be approximated by $\mu=c_0n^{\gamma_0}(1+c_1n^{\gamma_1})$,[41] where c_0, c_1, γ_0, and γ_1 are constants, and $\int \mathrm{d}r|\Psi^2|=N$ denotes the number of atoms in the condensate. As in Ref. [36], we introduce a disk-shaped harmonic trap to the system with the strongly shortened axis along the z direction as follows:

$$V_{\rm ext}(r)=\frac{1}{2}m[{\omega_\perp}^2(x^2+y^2)+{\omega_z}^2z^2],\quad(\omega_\perp\ll\omega_z),$$

where ω_z and $\omega_\perp$ are the frequencies of the trap in the z direction and the transverse (x or y) direction, respectively. In combination with its modulus and phase, the order parameter takes the form of $\Psi=\sqrt{n}\exp(\mathrm{i}\phi)$, and then we can obtain a series of coupled equations for n and ϕ as

$$\frac{\partial n}{\partial t}+\frac{\hbar}{m}\boldsymbol{\nabla}\cdot(n\boldsymbol{\nabla}\phi)=0, \tag{2}$$

$$\frac{\partial\phi}{\partial t}+\frac{\hbar}{2m}\Big[(\boldsymbol{\nabla}\phi)^2-\frac{1}{\sqrt{n}}\boldsymbol{\nabla}^2\sqrt{n}\Big]+\frac{1}{\hbar}(V_{\rm ext}(r)+\mu)=0. \tag{3}$$

By introducing

$$(x,y,z)=a_z(x',\ \ y',\ \ z'),\ \ \ t=\omega_z^{-1}t',\ \ \ n=n_0n',$$

with

$$a_z=\sqrt{\hbar/m\omega_z},\ \ \ n_0=N/a_z^3,\ \ \ \mu=\hbar\omega_z\mu',$$

we arrive at the following dimensionless equations after dropping the primes:

$$\frac{\partial n}{\partial t}+\boldsymbol{\nabla}\cdot(n\boldsymbol{\nabla}\phi)=0, \tag{4}$$

$$\frac{\partial\phi}{\partial t}+\frac{1}{2}z^2+\frac{1}{2}\left(\frac{\omega_\perp}{\omega_z}\right)^2(x^2+y^2)+\frac{1}{2}\Big[(\boldsymbol{\nabla}\phi)^2-\frac{1}{\sqrt{n}}\boldsymbol{\nabla}^2\sqrt{n}\Big]+\mu=0. \tag{5}$$

The quantum pressure term $(-\boldsymbol{\nabla}^2\sqrt{n}/2\sqrt{n})$ appears on the left side of Eq. (5), which has a great effect on the dispersion of the system. In the disk-shaped trap, the value of $\omega_\perp/\omega_z$ is small enough, so we neglect the third term on the left-hand side of Eq. (5) here and later. According to Eq. (5), under such a consideration, it is easily found that the energy-level space in the z direction is much larger than the energy of atom–atom interaction, which means the quasi-2D condensate. Furthermore, we can see the motion of atoms in the z direction is frozen and governed by the ground-state wave function of the corresponding harmonic oscillator. Thus, the excitation can only propagate in the (x,y) plane. Based on the analysis above, we take $\sqrt{n}=A(x,y,t)G(z)$, and $\phi=-\rho t+\varphi(x,y,t)$, where ρ denotes the chemical potential of the ground state, and $G(z)$ satisfies the following well-known eigenvalue function of a 1D harmonic oscillator in quantum mechanics:

$$-\frac{1}{2}\frac{\mathrm{d}^2G}{\mathrm{d}z^2}+\frac{1}{2}z^2G=\nu G, \tag{6}$$

and its ground-state solution takes the form

$$G_0(z)=\exp(-z^2/2),$$

with the eigenvalue $\nu=1/2$. Substituting these identities into Eqs. (4) and (5), we obtain

$$\frac{\partial A}{\partial t}+\frac{\partial A}{\partial x}\frac{\partial\varphi}{\partial x}+\frac{\partial A}{\partial y}\frac{\partial\varphi}{\partial y}+\frac{1}{2}A\left(\frac{\partial^2\varphi}{\partial x^2}+\frac{\partial^2\varphi}{\partial y^2}\right)=0, \tag{7}$$

$$-\frac{1}{2}\left(\frac{\partial^2A}{\partial x^2}+\frac{\partial^2A}{\partial y^2}\right)+\left(-\rho+\frac{1}{2}\right)A+\left[\frac{\partial\varphi}{\partial t}+\frac{1}{2}\left(\frac{\partial\varphi}{\partial x}\right)^2+\frac{1}{2}\left(\frac{\partial\varphi}{\partial y}\right)^2\right]A+\frac{c_0}{\sqrt{2\gamma_0+1}}A^{2\gamma_0+1}+\frac{c_0c_1}{\sqrt{2\gamma_0+2\gamma_1+1}}A^{2\gamma_0+2\gamma_1+1}=0. \tag{8}$$

Aiming to derive Eqs. (7) and (8), we followed the same procedure as that in Refs. [36] and [47]. Specifically, we let $G(z)=G_0(z)$ and multiplied Eq. (5) by G_0^*, then integrated once with respect to z to eliminate the dependence on z. Actually we can generally multiply Eq. (5) by an arbitrary function in terms of $\exp(-z^2/b)$, with b being an arbitrary constant, so that the differences only lie in the coefficients of the terms with high powers of A. Since we only take the case of a thin-disk-shaped trap ($\omega_\perp\ll\omega_z$) into consideration, the trapping potential in the (x,y) plane is a slowly varying function of x and y. As a result, the size of condensate in the radial direction is much larger.

Now we begin to discuss the linear and nonlinear exciting properties of the system. Firstly, we consider the linear case. Let $A = u_0 + a(x, y, t)$ ($u_0 > 0$), with $(a, \varphi) = (a_0, \varphi_0)\exp[\mathrm{i}(k_1 x + k_2 y - \omega t)] + \text{c.c.}$, u_0, a_0, and φ_0 being constants, we derive the linear dispersion relation of Eqs. (7) and (8) as

$$\omega(k_1, k_2) = \pm\frac{1}{2}k(2\sqrt{2\gamma_0 + 2\gamma_1 + 1}c_0 c_1 u_0^{2\gamma_0+2\gamma_1} + k^2)^{1/2}, \quad (9)$$

where $k^2 = k_1^2 + k_2^2$. Equation (9) is a Bogoliubov-type linear excitation spectrum of a 2D system; it is also closely related to the quantum pressure of the system. At this point, we can also derive the sound speed of the system given by the formula based on the following relation between c, ω, k_1, and k_2:

$$c = \lim_{k\to 0}\left[\left(\frac{\partial\omega}{\partial k_1}\right)^2 + \left(\frac{\partial\omega}{\partial k_2}\right)^2\right]^{1/2} = \pm\frac{1}{2}(2\sqrt{2\gamma_0 + 2\gamma_1 + 1}c_0 c_1 u_0^{2\gamma_0+2\gamma_1})^{1/2}, \quad (10)$$

of which the concrete value depends on the real parameters c_0, c_1, γ_0, and γ_1.

2.2. Basic set of KPI equation

Next, we study the weak nonlinear excitations of the system by means of perturbation, which has been widely used to solve many physical issues.[42,43] For the long wavelength disturbance with a finitely small amplitude, we use the asymptotic expansion $A = u_0 + \epsilon^2(a^{(0)} + \epsilon^2 a^{(1)} + \cdots)$, $\varphi = \epsilon(\varphi^{(0)} + \epsilon^2\varphi^{(1)} + \cdots)$, where $a^{(j)}$ and $\varphi^{(j)}$ are assumed to be functions of the multiple-scale variables $\xi = \epsilon(x - ct)$, $\eta = \epsilon^2 y$, and $\tau = \epsilon^3 t$. The variable ϵ is a small parameter characterizing the relative amplitude of the excitation. Substituting them into Eqs. (7) and (8), we arrive at the following equations:

$$c\frac{\partial a^{(j)}}{\partial\xi} - \frac{1}{2}u_0\frac{\partial^2\varphi^{(j)}}{\partial\xi^2} = \alpha^{(j)}, \quad (11)$$

$$c_0 c_1\sqrt{2\gamma_0 + 2\gamma_1 + 1}u_0^{2\gamma_0+2\gamma_1}a^{(j)} - cu_0\frac{\partial\varphi^{(j)}}{\partial\xi} = \beta^{(j)}, \quad (12)$$

where $j = 0, 1, \ldots$, the concrete expression of $\alpha^{(j)}$ is omitted, and $\beta^{(j)}$ satisfies $\beta^{(j)} = 2c\int\alpha^{(j)}\mathrm{d}\xi$.

For the first order ($j = 0$), we obtain the smallest quantity $a^{(0)}$, and $\varphi^{(0)}$ satisfies $\varphi^{(0)} = (2c/u_0)\int\mathrm{d}\xi a^{(0)}$, where $a^{(0)}$ is a function to be determined. For the next order, the solvability condition results in the closed equation for $a^{(0)}$

$$\frac{\partial}{\partial\xi}\left(\frac{\partial a^{(0)}}{\partial\tau} + \frac{3c}{2u_0}a^{(0)}\frac{\partial a^{(0)}}{\partial\xi} - \frac{1}{8c}\frac{\partial^3 a^{(0)}}{\partial\xi^3}\right) + \frac{c}{2}\frac{\partial^2 a^{(0)}}{\partial\eta^2} = 0. \quad (13)$$

The fourth-order derivative term with respect to ξ and the second-order derivative term with respect to η have opposite signs.

Introducing

$$u = -4c^2\epsilon^2 a^{(0)}/u_0, \quad X = -(x - ct)/\sqrt[6]{2}, \quad Y = \sqrt{3}y/\sqrt[3]{2^4}c, \quad T = t/8\sqrt{2}c, \quad U = u/\sqrt[3]{4} \quad (14)$$

to Eq. (13), together with the definitions of ξ, η, and τ, we obtain

$$\frac{\partial}{\partial X}\left(\frac{\partial U}{\partial T} + 6U\frac{\partial U}{\partial X} + \frac{\partial^3 U}{\partial X^3}\right) - 3\frac{\partial^2 U}{\partial Y^2} = 0. \quad (15)$$

In contrast to the standard form of the KP equation in the following form:

$$(u_t + 6uu_x + u_{xxx})_x + 3\sigma^2 u_{yy} = 0,$$

where $u = u(x, y, t)$ is a scalar function, x and y are, respectively, the longitudinal and transverse spatial coordinates, subscripts x, y, and t denote partial derivatives, and $\sigma^2 = \pm 1$, we just find that our study satisfies $\sigma^2 = -1$, which means that equation (15) is the standard form of the KPI equation, differing a lot from the opposite condition that $\sigma^2 = 1$ (i.e., the KPII eqution).[44,45]

3. Exact solutions of the KPI equation

As is known, the KPI equation also has the lump soliton solutions localized in 2D space. At first, we study solutions of multi-lump solitons. Exact multi-lump solutions of the KPI equation can be obtained in several ways, and we write them in the Hirota form:[46]

$$U(X, Y, T) = 2\frac{\partial^2}{\partial X^2}\ln V(X, Y, T),$$

where V is defined as

$$V = \det\left[(X - 2k_{i\pm}Y + 12k_{i\pm}^2 T + \gamma_{i\pm})\delta_{i,l} - j\frac{1 - \delta_{i,l}}{k_{i\pm} - k_{l\pm}}\right],$$

and $\delta_{i,l}$ is the Kronecker symbol. Here $i, l = 1, 2, \ldots$, $N \equiv 2M$, and M specifies the number of solitons. The parameters $k_{i\pm} = k_{i\mathrm{R}} \pm jk_{i\mathrm{I}}$ and $\gamma_{i\pm} = \gamma_{i\mathrm{R}} \pm j\gamma_{i\mathrm{I}}$

determine the amplitude (velocity) and the phase of each soliton. In particular, if $M = 1$, then

$$V = (\xi - 2k_{1\mathrm{I}}\eta)^2 + 4k_{1\mathrm{I}}^2\eta^2 + \frac{1}{4k_{1\mathrm{I}}^2},$$

$$U(X,Y,T) = 16\frac{-4(\xi - 2k_{1\mathrm{I}}\eta)^2 + 16k_{1\mathrm{I}}^2\eta^2 + 1/k_{1\mathrm{I}}^2}{[4(\xi - 2k_{1\mathrm{I}}\eta)^2 + 16k_{1\mathrm{I}}^2\eta^2 + 1/k_{1\mathrm{I}}^2]^2}, \quad (16)$$

where

$$\xi = X - 12(k_{1\mathrm{R}}^2 + k_{1\mathrm{I}}^2)T + \frac{\gamma_{1\mathrm{R}} + k_{1\mathrm{R}}\gamma_{1\mathrm{I}}}{k_{1\mathrm{I}}},$$
$$\eta = Y - 12k_{1\mathrm{R}}T + \frac{\gamma_{1\mathrm{I}}}{2k_{1\mathrm{I}}}.$$

Thus, we have obtained the one-lump solution of Eq. (15). In the case of $M = 2, 3, \ldots$, we can derive its multi-lump soliton solutions. For convenience, one-lump solution is also written in the following form:

$$U(X,Y,T) = \frac{4[-(X + aY + 3(a^2 - b^2)T)^2 + b^2(Y + 6aT)^2 + 1/b^2]}{[(X + aY + 3(a^2 - b^2)T)^2 + b^2(Y + 6aT)^2 + 1/b^2]^2}, \quad (17)$$

with a and b being real parameters. Thus, we obtain the density of the condensate corresponding to the lump-soliton solution of the KPI equation given below:

$$|\Psi^2| = u_0^2\mathrm{e}^{-z^2}[1 - \frac{\sqrt[3]{4}}{c^2}\frac{-[X + aY + 3(a^2 - b^2)T]^2 + b^2(Y + 6aT)^2 + 1/b^2}{\{[X + aY + 3(a^2 - b^2)T]^2 + b^2(Y + 6aT)^2 + 1/b^2\}^2}]^2. \quad (18)$$

From the solution obtained above, we know that the excitation is a 2D dip (localized in the x and y directions), which is excited on the condensate background (represented by $u_0^2\exp(-z^2)$). Additionally, we can obtain the velocity of the dark lump

$$V_{\mathrm{s}} = \left\{c^2\left[1 - \frac{\sqrt[6]{2}}{8\sqrt{2}c^2}(p_{\mathrm{r}}^2 + p_{\mathrm{i}}^2)\right]^2 + \left(\frac{2^{7/3}p_{\mathrm{r}}}{8\sqrt{6}}\right)^2\right\}^{1/2}, \quad (19)$$

where c was defined by Eq. (10), and p_{r} and p_{i} are arbitrary real constants. However, the validity of the KPI equation requires small values of p_{r} and p_{i}.

Moreover, the line-soliton solutions of the KPI equation have been studied extensively in the past few years.[47–49] The one-line-soliton solution is given by

$$U(X,Y,T) = 2k^2\mathrm{sech}^2\{k[X + \lambda Y - (4k^2 - 3\lambda^2)T + \delta_0]\}, \quad (20)$$

and the two-line-soliton solution expressed in terms of Hirota's notation is given by

$$U(X,Y,T) = 2\frac{\partial^2}{\partial X^2}\ln F(X,Y,T), \quad (21)$$

where

$$F(X,Y,T) = 1 + \exp(\eta_1) + \exp(\eta_2) + \exp(\eta_1 + \eta_2 + A_{12}),$$

and

$$\eta_i = 2k_i[X + \lambda_i Y - (4k_i^2 - 3\lambda_i^2)T] + \delta_0, \ (i = 1, 2),$$

$$\exp(A_{12}) = \frac{4(k_1 - k_2)^2 + (\lambda_1 - \lambda_2)^2}{4(k_1 + k_2)^2 + (\lambda_1 - \lambda_2)^2}.$$

For simplicity, let

$$k_1 = k_2 = k, \ \ \lambda_1 = -\lambda_2 = \lambda,$$

we obtain the two-soliton solution with the same amplitude

$$U(X,Y,T) = K^2[\mathrm{e}^{KX+LY+\omega T} + \mathrm{e}^{KX-LY+\omega T} + A_0\mathrm{e}^{3KX+LY+3\omega T} + A_0\mathrm{e}^{3KX-LY+3\omega T} + 4A_0\mathrm{e}^{2KX+2\omega T}](1 + \mathrm{e}^{KX+LY+\omega T} + e^{KX-LY+\omega T} + A_0\mathrm{e}^{2KX+2\omega T})^{-2}, \quad (22)$$

where $A_0 = \lambda^2/(\lambda^2 + 4k^2)$, $K = 2k$, $L = 2k\lambda$, and $\omega = 8k(3\lambda^2 - k^2)$. Introducing the transformation of Eq. (14) into Eq. (22), we obtain the asymptotic behaviour of the two-soliton solution of Eq. (22) as x and y approach infinity at a fixed time t. There are four cases of $x \to \pm\infty$ and $y \to \pm\infty$, and hence we use $u^{(1)}$, $u^{(2)}$, $u^{(3)}$, and $u^{(4)}$ to represent the two-line-soliton solutions of four cases.

It is found that under the condition that $x \to -\infty$ and $y \to +\infty$, the limit $u^{(1)}$ is given by

$$u^{(1)} = \frac{K^2}{2}\mathrm{sech}^2\frac{1}{2}\left(-K\frac{x - ct}{\sqrt[6]{2}} - L\frac{\sqrt{3}y}{2\sqrt[3]{2}c} + \omega\frac{t}{8\sqrt{2}c} + \delta\right), \quad (23)$$

and for the case that $x \to -\infty$ and $y \to -\infty$, $u^{(2)}$ is given by

$$u^{(2)} = \frac{K^2}{2}\operatorname{sech}^2\frac{1}{2}\Big(-K\frac{x-ct}{\sqrt[6]{2}} + L\frac{\sqrt{3}y}{2\sqrt[3]{2}c} + \omega\frac{t}{8\sqrt{2}c} + \delta\Big), \tag{24}$$

where $\delta = \ln A_0$. For $x \to +\infty$ and $y \to +\infty$, $u^{(3)}$ is given by

$$u^{(3)} = \frac{K^2}{2}\operatorname{sech}^2\frac{1}{2}\Big(-K\frac{x-ct}{\sqrt[6]{2}} + L\frac{\sqrt{3}y}{2\sqrt[3]{2}c} + \omega\frac{t}{8\sqrt{2}c}\Big). \tag{25}$$

For $x \to +\infty$ and $y \to -\infty$, $u^{(4)}$ is given by

$$u^{(4)} = \frac{K^2}{2}\operatorname{sech}^2\frac{1}{2}\Big(-K\frac{x-ct}{\sqrt[6]{2}} - L\frac{\sqrt{3}y}{2\sqrt[3]{2}c} + \omega\frac{t}{8\sqrt{2}c}\Big). \tag{26}$$

4. Discussion and conclusion

Based on the analysis above, we can gain the one-lump-soliton solution and the corresponding atomic number density of the system, as shown in Figs. 1 and 2, respectively.

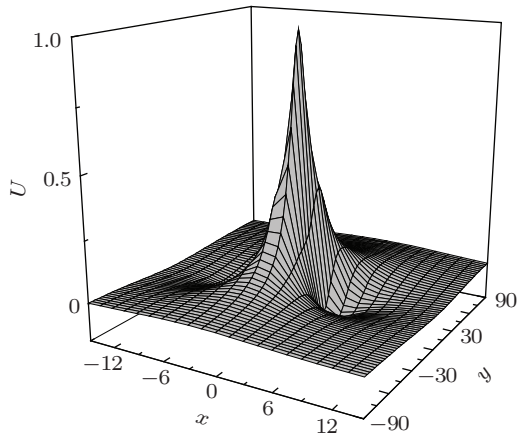


Fig. 1. Profile of the one-lump-soliton solution of the KPI equation at $t = 0$.

Figure 1 shows the profile of the single-lump solution of the KPI equation in (x, y) plane at $t = 0$. We note that the solution decays as $x^2 \to \infty$ and $y^2 \to \infty$. By describing the single-lump soliton at nonzero t,

we find that the first and fourth cases correspond to the same soliton whose phase has been changed by $\delta = \ln A$ upon interaction. Figure 2 shows the profile of condensate density $P = |\Psi|^2$ corresponding to the single-lump solution at $t = 0$. It is obviously seen that the lump soliton stably propagates on the (x, y) plane.

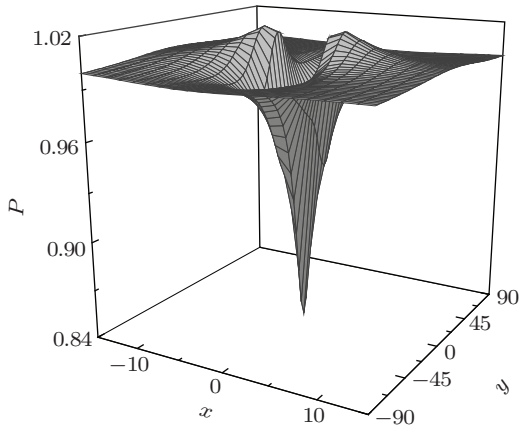


Fig. 2. Profile of the corresponding condensate density $P = |\Psi|^2$ of the one-lump-soliton solution of the KPI equation at $t = 0$.

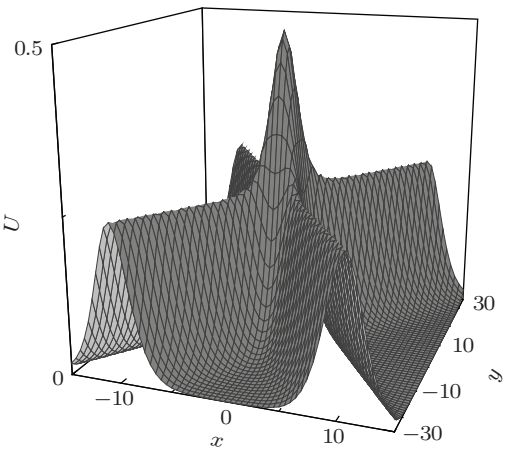


Fig. 3. Profile of the two-line-soliton solution at $t = 0$ for $k = 0.5$ and $\lambda = 5$.

For the two-line-soliton solution of the KPI equation, we have discussed the soliton solution with same amplitude. The wave function and condensate density in the (x, y) plane are shown in Figs. 3 and 4, respectively, with $k = 0.5$ and $\lambda = 5$. We have obtained limited results of the two line-soliton solution under four different cases of $x \to \pm\infty$ and $y \to \pm\infty$. We find that the first and fourth cases correspond to one soliton whose phase change can be counted as $\delta = \ln A$ after soliton interaction. Thus, we know the soliton properties such as the amplitude, propagating velocity, and width remain unchanged after interaction. Similarly, the second and third cases correspond to another soliton with its phase being the only changed soliton parameter after the interaction. We can also note that the phase change between the first and fourth solitons (or the second and third cases) depends on the angle

θ between two solitons. Suppose $2\theta = \arctan(\lambda/k)$, then if $\lambda \ll k$, i.e., θ is small enough, the phase shifts by an amount of $\delta \to -\infty$. By contrast, if $\lambda \gg k$, namely the angle $\theta \to \pi/2$, the phase change tends to be zero, which is in good agreement with the situation for the BEC system.[47]

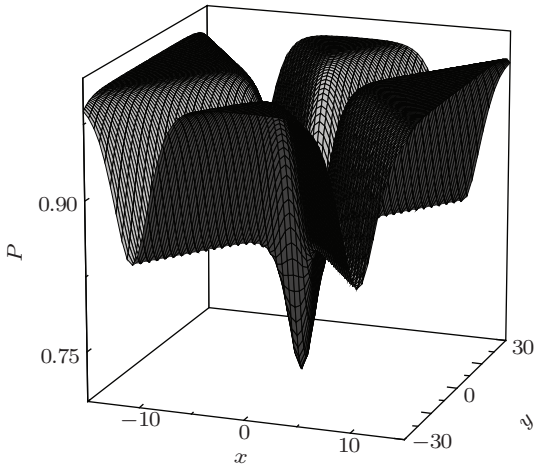


Fig. 4. Profile of the condensate density $P = |\Psi|^2$ corresponding to the two-line-soliton solution at $t = 0$ for $k = 0.5$ and $\lambda = 5$.

In the deep BEC regime where $\gamma_0 = 1$, $\gamma_1 = 1/2$, $c_0 = d_0\eta^{-1}$, and $c_1 = d_1\eta^{-5/2}$, we choose $d_0 = 3.42$, $d_1 = 15.88$, and $u_0 > 0$.[29] In the unitarity regime where $\gamma_0 = 2/3$, $\gamma_1 = -1/3$, $c_0 = d_0'$, and $c_1 = d_1'\eta$, we choose $d_0' = 1.40$, $d_1' = 4.39$, and $u_0 > 0$.

Figure 5 shows the dependence of sound speed c on $\eta = 1/k_{\rm F}a_{\rm sc}$ in 2D superfluid Fermi gases for different values of u_0 in the unitarity regime. It is obviously seen that the sound speed increases as $\eta = 1/k_{\rm F}a_{\rm sc}$ and u_0 increase, and decreases as the condensate density n and s-wave scattering length increase, whose case is also inconsistent with that of the 1D superfluid Fermi system,[50], but quite different from that in Ref. [34]. The main reason lies in the higher-order bulk chemical potential μ used in our work. We also note that the sound speed in a 2D superfluid Fermi system is higher than that in a 1D Fermi system in the case of unitarity, which agrees well with that in Ref. [34].

Figure 6 shows the dependence of the sound speed of 2D superfluid Fermi gases on the interaction parameter $\eta = 1/k_{\rm F}a_{\rm sc}$ for different values of u_0 in the deep BEC regime. We note that the sound speed decreases as the value of $\eta = 1/k_{\rm F}a_{\rm sc}$ increases, i.e., the sound speed increases as the condensate density n and s-wave scattering length increases. Similarly, the variable c increases as u_0 increases, and the sound speed in a 2D superfluid Fermi system is larger than that of a 1D Fermi system in the deep BEC regime, which is in good agreement with that of the 1D superfluid Fermi gases.[34,50] Moreover, we find the sound speed of 2D superfluid Fermi system is larger than that of the 1D system where the confinement is applied in two directions. Such conclusions have also been obtained in Refs. [34] and [36] for both Fermonic and Bosonic systems.

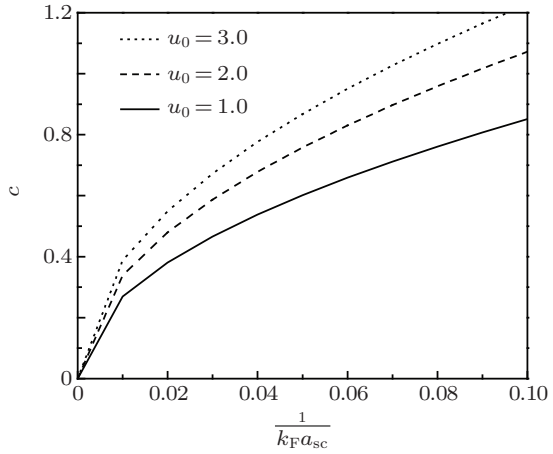


Fig. 5. Dependence of the sound speed of the superfluid Fermi gases on the interaction parameter $\eta = 1/k_{\rm F}a_{\rm sc}$ for different values of u_0 in the case of unitarity.

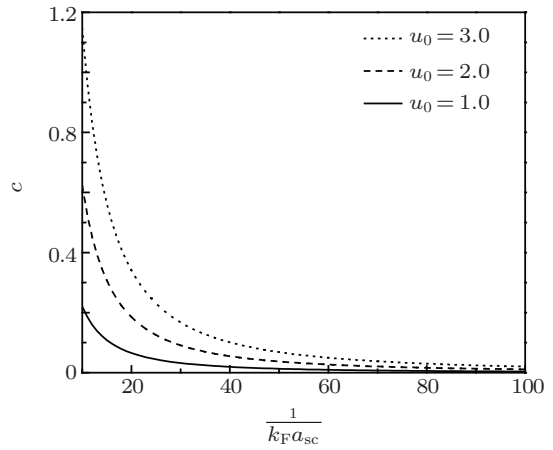


Fig. 6. Dependence of the sound speed of the superfluid Fermi gases on the interaction parameter $\eta = 1/k_{\rm F}a_{\rm sc}$ for different values of u_0 in the deep BEC regime.

Figures 7 and 8 show the variation of the lump propagating velocity (given by Eq. (19)) with respect to the interaction parameter $\eta = 1/k_{\rm F}a_{\rm sc}$ for different values of u_0 in the cases of the unitarity and the deep BEC regime, respectively. Obviously, the dependence of the lump propagating velocity on the interaction parameter $\eta = 1/k_{\rm F}a_{\rm sc}$ is the same as that of the sound speed in superfluid Fermi gases: the lump propagating

velocity in the case of unitarity decreases with the increasing wave number or the condensate density; the lump velocity in the unitarity, which is just the opposite to its couterpart in the deep BEC regime, decreases with the increasing s-wave scattering length. However, for a certain value of $\eta = 1/k_{\rm F}a_{\rm sc}$, the value of lump velocity is smaller than the sound speed of the system, which is in good agreement with the results in Ref. [34]. Compared with the propagating of the dark soliton of 1D superfluid Fermi gases,[50] the lump velocity is also much larger for the disk-shaped harmonic confinement only applied in the axial direction (z direction), which agrees well with Refs. [34] and [51].

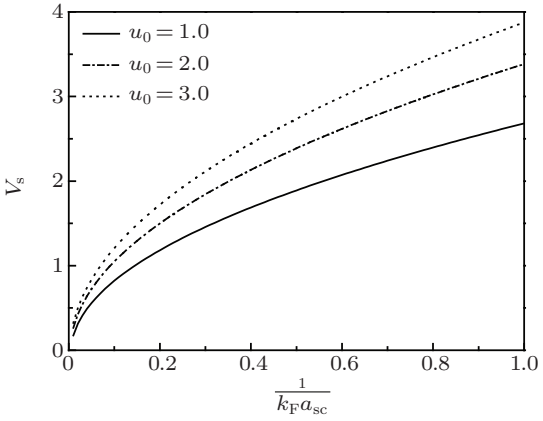


Fig. 7. Variation of the lump propagating velocity with respect to the interaction parameter $\eta = 1/k_{\rm F}a_{\rm sc}$ for different values of u_0 in the case of unitarity.

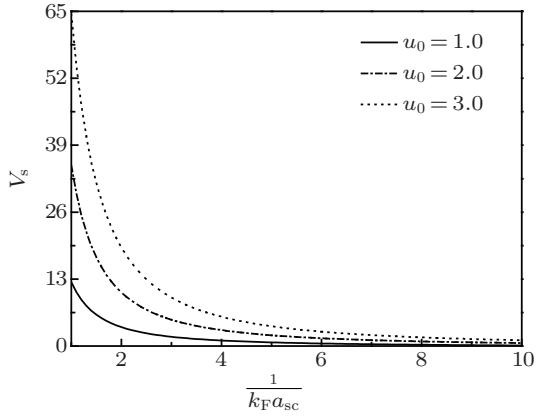


Fig. 8. Variation of the lump propagating velocity with respect to the interaction parameter $\eta = 1/k_{\rm F}a_{\rm sc}$ for different values of u_0 in the deep BEC regime.

On the basis of the conclusions and figures we obtained, there exist quite different characteristics in 2D superfluid Fermi gases for different regimes. By comparing our results with some other research results, both common and different properties have been displayed. The main reason for the distinctions lies in the higher-order bulk chemical potential $\mu = c_0 n^{\gamma_0}(1 + c_1 n^{\gamma_1})$ introduced in our study, with c_0 and c_1 being the parameters closely related to the interaction parameter $\eta = 1/k_{\rm F}a_{\rm sc}$. Compared with the bulk chemical potential $\mu = Cn^{\gamma}$ applied elsewhere, the parameters c_0 and c_1 in our model are in different forms of dependence on $\eta = 1/k_{\rm F}a_{\rm sc}$ for different regimes, which differs a lot from C. Furthermore, it can be easily noted that the limit values of γ_0 and γ_1 in different superfluid regimes differs from that of γ. Undoubtedly, different characteristics and results will be presented.

References

[1] O'Hara K M, Hemmer S L, Gehm M E, Granade S R and Thomas J E 2002 *Science* **298** 2179

[2] Jochim S, Bartenstein M, Altmeyer A, Hendl G, Riedl S, Chin C, Denschlag J H and Grimm R 2003 *Science* **302** 2101

[3] Greiner M, Regal C A and Jin D S 2003 *Nature* **426** 537

[4] Bartenstein M, Altmeyer A, Riedl S, Jochim S, Chin C, Denschlag J H and Grimm R 2004 *Phys. Rev. Lett.* **92** 203201

[5] Astrakharchik G E, Boronat J, Casulleras J and Giorgini S 2004 *Phys. Rev. Lett.* **93** 200404

[6] Dong H and Ma Y L 2009 *Chin. Phys.* B **18** 715

[7] Heiselberg H 2004 *Phys. Rev. Lett.* **93** 040402

[8] Wu B, Liu J and Niu Q 2002 *Phys. Rev. Lett.* **88** 034101

[9] Dalfovo F, Giorgini S, Pitaevskii L and Stringari S 1999 *Rev. Mod. Phys.* **71** 463

[10] Zhang J M, Cui F C, Zhou D L and Liu W M 2009 *Phys. Rev.* A **79** 033401

[11] Zhang X F, Hu X H, Liu X X and Liu W M 2009 *Phys. Rev.* A **79** 033630

[12] Liu J, Zhang C, Raizen M G and Niu Q 2006 *Phys. Rev.* A **73** 013601

[13] Liu J, Wang W, Zhang C, Niu Q and Li B 2005 *Phys. Rev.* A **72** 063623

[14] Li B, Li Y Q, Chen Y, Zhang X F and Liu W M 2008 *Phys. Rev.* A **78** 023608

[15] Wu Y and Yang X X 2003 *Phys. Rev.* A **68** 013608

[16] Burger S, Bongs K, Dettmer S, Ertmer W, Sengstock K, Sanpera A, Shlyapnikov G V and Lewenstein M 1999 *Phys. Rev. Lett.* **83** 5198

[17] Dutton Z, Budde M, Slowe C and Hau L V 2001 *Science* **293** 663

[18] Wen W, Shen S Q and Huang G X 2010 *Phys. Rev.* B **81** 014528

[19] Manini N and Salasnich L 2005 *Phys. Rev.* A **71** 033625

[20] Hu H, Minguzzi A, Liu X and Tosi M P *Phys. Rev. Lett.* **93** 190403

[21] Salasnich L, Manini N and Toigo F *Phys. Rev.* A **77** 043609

[22] Spuntarelli A, Pieri P and Strinati G C 2007 *Phys. Rev. Lett.* **99** 040401

[23] Wu X, Deng D and Guo Q 2011 *Chin. Phys.* B **20** 084201
[24] Yang S J, Wu Q S, Zhang S N and Feng S P 2008 *Phys. Rev.* A **77** 033621
[25] Yang S J, Wu Q S, Feng S P, Wen Y C and Yu Y 2008 *Phys. Rev.* A **77** 035602
[26] Yu H, Peng J and Jin B 2010 *Chin. Phys.* B **19** 087203
[27] Wang P, Fu Z, Chai S and Zhang J 2011 *Chin. Phys.* B **20** 103401
[28] Scott T F, Ballagh R J and Burnett K 1998 *J. Phys.* B **31** L329
[29] Wang W Y, Duan W S, Sun J A and Yang Y 2011 *Eur. Phys. J.* B **84** 283
[30] Zhou L, Kong L B and Zhan M S 2008 *Chin. Phys.* B **17** 1601
[31] Ancilotto F, Salasnich L and Toigo F 2009 *Phys. Rev.* A **79** 033627
[32] Adhikari S K and Salasnich L 2008 *Phys. Rev.* A **78** 043616
[33] Liu C, Hu K, Hu T and Tang Y 2011 *Chin. Phys.* B **20** 010309
[34] Wen W and Huang G 2009 *Phys. Rev.* A **79** 023605
[35] Wu Y and Deng L 2004 *Phys. Rev. Lett.* **93** 143904
[36] Huang G X and Zhu S H 2002 *Chin. Phys. Lett.* **19** 17
[37] Huang G X, Velarde M G and Makarov V A 2001 *Phys. Rev.* A **64** 013617
[38] Huang G X, Makarov V A and Velarde M G 2003 *Phys. Rev.* A **67** 023604
[39] Görlitz A, Vogells J M, Leanhardt A E, Raman C, Gustavson T L, AboShaeer J R, Chikkatur A P, Gupta S, Inouye S, Rosenband T and Ketterle W 2001 *Phys. Rev. Lett.* **87** 130402
[40] Adhikari S K, Lu H and Pu H 2009 *Phys. Rev.* A **80** 063607
[41] Cao S, Ma Y and Huang G 2009 *Phys. Rev.* A **79** 013620
[42] Cheng X P, Lin J and Yao J M 2009 *Chin. Phys.* B **18** 0391
[43] Ren X C and Guo L X 2008 *Chin. Phys.* B **17** 2491
[44] Ablowitz M J and Clarkson P A 1991 *Solitons, Nonlinear Evolution Equations and Inverse Scattering* (Cambridge: Cambridge University Press)
[45] Gino B and Pelinovsky D E 2008 *Scholarpedia* **3** 6539
[46] Berger K M and Milewski P A 2000 *SIAM J. Appl. Math.* **61** 731
[47] Duan W S, Chen J H, Yang H J, Shi Y R and Wang H Y 2006 *Chin. Phys. Lett.* **23** 2000
[48] Shi Y R, Zhang J, Yang H J, Duan W S and Lonngren K E 2011 *Chin. Phys.* B **20** 015205
[49] Dinkel J N, Setzer C, Rawal S and Lonngren K E 2001 *Chaos Soliton. Fract.* **12** 91
[50] Xu Y X and Duan W S 2011 *Chin. Phys. Lett.* **28** 125203
[51] Wen W and Huang G 2007 *Phys. Lett.* A **362** 331